Water Resour Manage (2016) 30:5455–5478
DOI 10.1007/s11269-016-1500-x

A Sub-Catchment Based Approach for Modelling Nutrient Dynamics and Transport at a River Basin Scale

Md Jahangir Alam[1] · **Dushmanta Dutta**[2]

Received: 13 August 2015 / Accepted: 8 September 2016 /
Published online: 9 October 2016

Abstract The prediction of nutrient pollution at realistic details is difficult due to lack of proper description of inherent processes in modelling tools. To overcome that this study has adopted a process based approach to build a semi-distributed model to simulate nutrient pollution in changing environment. The model was built to describe: (1) nutrient generation process in the catchment with consideration of different aspects of external and internal sources, (2) nutrient release from surface to the waterways via runoff and soil erosion, and (3) in-stream transport and chemical reaction process. The key novelty of this research is the linking of the nutrient generation process with transport mechanism for modelling nutrient dynamics at a basin scale. A flow capacity based approach was introduced to determine nutrient export from catchment to the waterways, which was useful to achieve the high resolution outputs from the model. The model performed reasonably well to represent the behaviour of nutrient in high flow events as well as in seasonal flow in two catchments located in distinct hydro-climatic regions. The study has shown that the nutrient model is suitable for predicting actual nutrient pollution in rivers for both high flow and seasonal flow under different hydro-climatic conditions. By simulating organic and inorganic nutrients separately, the model allows to estimate river water quality status in detail.

Keywords Nutrient pollution · Process-based modelling · Soil erosion · Catchment and in-stream process · River basin

1 Introduction

The quantification of nutrient pollution is one of the major issues in water resources management (Panagopoulos et al. 2011; Dutta et al. 1998). Over the past few decades, nutrient

✉ Dushmanta Dutta
Dushmanta.dutta@csiro.au

[1] University of Southern Queensland, Darling Heights, QLD, Australia

[2] CSIRO Land and Water, Canberra, ACT, Australia

pollution has impacted river water quality mainly for land use change, agricultural practices and increases of pollution sources (Whitehead et al. 1998a; Guse et al. 2015). Accounting the inherent processes is necessary for modeling the catchment behavior and predicting the pollution level at higher spatio-temporal resolutions, which is the main focus in this research.

Mostly the current modelling tools are conceptual in nature, developed for planning best management practice. This type of models are suitable for estimating the nutrient loads on an annual basis. They do not account hydrologic response and transport processes hence are unable to predict the nutrient level in higher spatio-temporal resolutions. Some of the tools have been improved or extended to predict nutrient level at a monthly or, daily time scale, such as, modelling tool E2 (Perraud et al. 2005) and Water and Contaminant Analysis and Simulation Tools (WaterCAST) (Cook et al. 2009). Similar conceptual models were developed for European catchments such as Modelling Nutrient Emissions in River Systems (MONERIS) (Venohr et al. 2011). Such models are comparatively simple to build (Tzoraki et al. 2014). However, using simple methods such as Event Mean Concentration (EMC) method or rate based approach the prediction of nutrient releases cannot be achieved at realistic details in changing environment. To overcome the situation this study has adopted a process-based nutrient modeling approach, which was emphasized in many studies. For example, a national level Australian study highlighted that due to the unavailability of proper models the effects of upstream flow processes and in-stream mechanisms on blue green algal growth remained unknown for many inland rivers in Australia (Croke and Young 2001).

A number of process-based nutrient models are reported in literature such as Integrated Catchment Model INCA-N and INCA-P ((Whitehead et al. 1998a, 1998b; Wade et al. 2002), DAISY- a soil/crop/atmosphere model (Hansen et al. 1990; Abrahamsen and Hansen 2000), Nitrogen Modelling system (NMS) (Lunn et al. 1996), the Hydrologic Simulation Program-Fortran (HSPF) (Wang et al. 2015a, b). The semi-distributed process based models INCA-N and INCA-P (Wade et al. 2002) provide output of nitrate and soluble reactive phosphorus at weekly interval in a river network system. Such models do not consider soil-erosion process in transport modelling. However, the soil bound nutrient could be an important source of nutrients such as Australian catchments (Croke 2002). The INCA is also unable to predict transient peaks due to poorly defined internal processes (Dise 2004). A greater ability was achieved in the coupling of process based field scale model DAISY and distributed hydrological model MIKESHE (Abbott et al. 1986). The use of MIKESHE/DAISY was limited to vertical transport and groundwater flow modelling for macro pore flow analysis (Refsgaard et al. 1999). Similar developments were undertaken in other process based hydrological model such as NMS model, which is a combination of the field-scale nitrogen model EPIC (Jones et al. 1991) and the catchment-scale flow and transport modelling system SHETRAN (Abbott et al. 1986). Although many of these process-based watershed models aimed to incorporate catchment process in simulating nutrient fate and transport, broadly they ignored the nutrient transport process with overland flow except few cases such as the sediment based nutrient release was considered in WATFLOOD model (Kouwen 1999; Leon et al. 2001).. The Soil and Water Assessment Tool (SWAT) (Arnold et al. 1998) is a similar type of model as WATFLOOD. MIKE11 (DHI 2002; Radwan et al. 2003), Water Quality Analysis Simulation Program (WASP) (Wagenschein and Rode 2008) or EFDC (Wu and Xu 2011) are detailed models but are mainly designed for water quality modelling of the receiving water such as river, lake or estuary. To overcome the limitations of the existing modelling approaches, this study aimed to incorporate: 1) representation of land use process, 2) mechanism on linking nutrient release from surface to the waterways through different pathways, and 3) description

of in-stream transport processes in a newly developed model. A sub-catchment based approach is trialled to test the suitability of the different components. The research was aimed at developing and implementing a process-based nutrient model at an hourly time-step by incorporating the above-mentioned three attributes and demonstrating its suitability in catchment scale nutrient simulation through real-world applications.

This paper describes the sub-catchment based nutrient model and its applications in two distinct hydro-climatic regions in Japan and Australia for producing various nutrient fluxes at a basin scale.

2 Modelling Approach

The nutrient model was built within an existing process-based and distributed hydrological model called IISDHM, (Jha et al. 2000; Dutta et al. 2000, 2006; Asokan and Dutta 2008; Dutta and Nakayama 2009; Kabir et al. 2011). There are advancements made in alternative hydrological modelling approach using artificial neural network and optimizing techniques such as genetic algorithm (Taormina and Chau 2015; Saeidifarzad 2014; Wu et al. 2009; Chen et al. 2015; Chau and Wu 2010). However, such models are based on analysis of historical data, which are out of the scope. Hence IISDHM is chosen as it is a robust model for deterministic modelling similar to other distributed hydrological models such as MIKESHE. IISDHM mathematically represents the key components of the hydrologic cycle using physical governing equations and then simulates the movement of water using the principles of conservation of mass and momentum. The hydrologic components are grouped into five distinct modules: (i) Interception and evapotranspiration simulation, (ii) Unsaturated zone flow simulation, (iii) Saturated zone flow simulation, (iv) Overland flow simulation and (v) Channel network flow simulation. The IISDHM was used to simulate catchment runoff and estimate river discharges. The model solves Saint-Venant's equations for continuity and momentum to compute surface and river flow. The kinematic wave method was used to approximate flow using an explicit finite difference solution scheme. The explicit model is conditionally stable by satisfying the Courant number (Chow et al. 1988). The IISDHM provides input of hydrologic flow for sub-catchment based modelling. Figure 1 shows the conceptual framework of the integrated model.

3 Catchment Nutrient Model

The catchment nutrient model estimates inorganic soluble nutrient release from different land uses (Alam and Dutta 2013). The net nutrient generation is estimated based on generation rate by accounting transformation process in the soil layer under different soil moisture conditions. The nutrient module includes both nitrogen (N) and phosphorous (P) models. The N model estimates the rate of net mineralization of N, denitrification and nitrate (using the equations for different processes as shown in Table 1). The P model estimates the rate of net mineralization of P taking into account various processes in the soil including the adsorption and desorption of inorganic P and weathering and precipitation of mineral P, and the output is inorganic soluble reactive P (PO_4-P). The equations for different processes included in the P model are shown in Table 1.

The soil moisture index (SMI) is determined based on the function of soil moisture deficit (SMD) in the soil. SMI varies from 0 to 1. It is zero when the deficit is maximum, (i.e.,

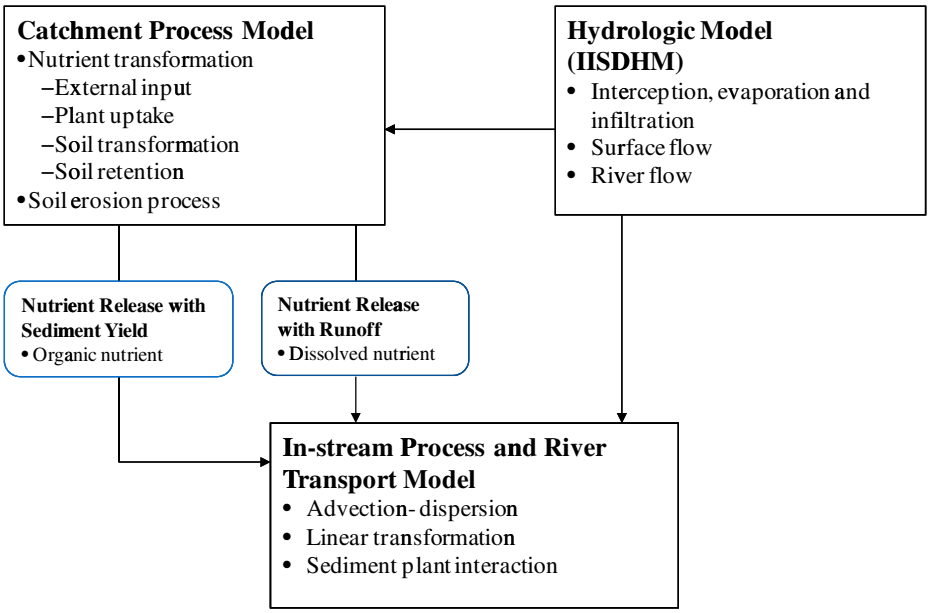

Fig. 1 The conceptual model framework

$SMD = SMD_{Max}$) and 1 when the soil is in saturation. *SMI* and *SMD* have been calculated from the following equations (Whitehead et al. 1998a; Finkele et al. 2006):

$$\frac{dSMD}{dt} = -P_{eff} + ET \tag{8}$$

$$SMI = \frac{SMD_{\max} - SMD}{SMD_{\max}} \tag{9}$$

Where

P_{eff} (rain-interception-runoff)	Effective rainfall
ET	Evapotranspiration.

Using Table 1, the final equations for soluble nutrients at any time t can be expressed as:

$$\frac{d}{dt}(NH_4{-}N)_t = \frac{d}{dt}(Ext_{N_{NH4}} + NetN_{Mina} - N_{NH_4}Uptake) \tag{10}$$

$$\frac{d}{dt}(NO_3{-}N)_t = \frac{d}{dt}\left(Ext_{N_{NO_3}} + Nitrification - NO_3Uptake - Denitrification\right) \tag{11}$$

$$\frac{d}{dt}(PO_4{-}P)_t = \frac{d}{dt}(Ext_P + NetP_{Mina} - PUptake) \tag{12}$$

Where, NH_4-N, NO_3-N and PO_4-P are ammonium, nitrate and dissolved phosphate, respectively; Ext_{NH4},Ext_{NO3} and Ext_P are external inputs of N_{NH4},N_{NO3} and P respectively, which may include fertilizer application, atmospheric deposition or sewage disposal or other forms of input depending on catchment characteristics.

Table 1 Equations of nitrogen and phosphorus transformation process in soil layer (Whitehead et al. 1998a)

Nitrogen transformation process	
Process	Equations
Plant Uptake	$\frac{d}{dt}N_{uptake} = C_{Nup}u_iX_N$ (1) Where, $C_{N\ up}$ = Nitrogen uptake rate of plant (day^{-1}), u_i = plant growth index, X_N = amount of ammonium and nitrate
Mineralization-immobilization	$\frac{d}{dt}(NetN_{Mina}) = C_{Nmina}SMI - C_{Nimm}X_{Namm}$ (2) Where, $C_{N\ mina}$ = Nitrogen mineralization rate (g day^{-1}), SMI = soil moisture index, $C_{N\ imm}$ = Nitrogen immobilization rate (day^{-1}), X_{amm} = amount of mineralized N
Nitrification	$\frac{d}{dt}Nitrification = C_{nitri}X_{NH_4-N}$ (3) Where, C_{nitri} = Nitrification rate (day^{-1}), X_{NH_4-N} = amount of Ammonium N
Denitrification	$\frac{d}{dt}Denitrifcation = C_{deni}X_{NO_3-N}$ (4) Where, C_{deni} = Denitrification rate (day^{-1}), X_{NO_3-N} = amount of Nitrate N
Temperature correction	$C_n = 1.047^{(\theta_s-20)}C_r$ (5) Where, C_n = rate of reaction (day^{-1}), C_r = rate of reaction (day^{-1}) at 20 °C, θ_s = Soil temperature (°C)
Phosphorus transformation process	
Process	Equations
Plant Uptake	$\frac{d}{dt}P_{Uptake} = C_{Pup}u_iX_{PO_4-P}$ (6) Where, CP up = Phosphorus uptake rate of plant (day-1), ui = plant growth index, X_{PO_4-P} = amount of Phosphate P
Mineralization-immobilization	$\frac{d}{dt}(NetP_{Mina}) = C_{Pmina}SMI - C_{pimm}X_{PO_4-P}$ (7) Where, Cp mina = Phosphorous mineralization rate (mg day-1), SMI = Soil moisture index, Cp imm = Phosphorous immobilization rate (day-1), X_{PO_4} = amount of reactive or phosphate P

The nutrients build up on the catchment surface through generation processes and are released with runoff. The release depends on the function of runoff. With this hypothesis, an export coefficient based nutrient release was introduced, which is a function of flow as shown in Eqs. (13–15).

$$\frac{d}{dt}(NH_4-N)_{release} = \frac{d}{dt}(NH_3-N)_t * U_w \tag{13}$$

$$\frac{d}{dt}(NO_3-N)_{release} = \frac{d}{dt}(NO_3-N)_t * U_w \tag{14}$$

$$\frac{d}{dt}(PO_4-P)_{release} = \frac{d}{dt}(PO_4-P)_t * U_w \tag{15}$$

The export coefficient U_W has been defined as below.

$$U_W = aQ^b \tag{16}$$

Where

a coefficient for soil and land cover effects

b power factor
Q flow in m^3/s.

3.1 Soil Erosion and Sediment Yield Models

The nutrient model includes the soil erosion and sediment yield model to compute soil bound nutrient (Organic N and P) release associated with soil erosion process. After estimating sediment load from each sub-catchment, soil bound nutrient release is calculated by multiplying the nutrient content with sediment load.

The estimation of soil erosion and sediment yield was carried out using Universal Soil Loss Equation (USLE) (Weischmer and Smith 1978) based models RUSLE (Renard et al. 1991, 1996) and MUSLE (Williams 1975; Williams and Berndt 1977). The RUSLE can be expressed by Eq. (17).

$$A_s = RKLSC_mP_s \tag{17}$$

Where

A_s Average annual soil loss predicted (ton ha^{-1})
R Rainfall runoff erosivity factor (MJ mm ha^{-1} h^{-1})
K Soil erodibility factor (ton ha hr MJ^{-1} ha^{-1} mm^{-1})
L Slope length factor
S Slope steepness factor
C_m Cover management factor
P_s Support practice factor.

The method is suitable for sub-catchment scale analysis (Weischmer and Smith 1978) and Bhattarai and Dutta (2008) demonstrated its suitability for estimating soil erosion at a monthly time scale. The fraction of the total amount of soil erosion, at the catchment outlet, is determined by multiplying the soil erosion with the term called soil delivery ratio. The soil delivery ratio is determined using the following equation (Bhattarai and Dutta 2007).

$$D_R = \exp\left(-\gamma \sum_{i=1}^{m} \frac{l_i}{a_{Li} S_i^{0.5}}\right) \tag{18}$$

Where

D_R Soil delivery ratio
i catchment cell
γ a constant for given catchment
a_L a constant for land use type
S surface slope
l the travel distance.

The Modified Universal Soil Loss Equation MUSLE (Williams 1975; Williams and Berndt 1977) was used for the upper catchment of the Latrobe River, which is as below.

$$S_y = a_1 (QV)^{b_1} KLSC_mP_s \tag{19}$$

Where

S_y	sediment yield
Q	discharge ($m^3\ s^{-1}$)
V	Volume in (m^3)
a_1 and b_2 constants	11.8 and 0.56 respectively
K	Soil erodibility factor
L	Slope length factor
S	Slope steepness factor
C_m	Cover management factor
P_s	Support practice factor.

3.2 Estimation of Soil Bound Nutrients

The soil bound nutrients were estimated using the following equations (Leon et al. 2001).

$$N_{SED} = N_{SCN} Y_{SED} ER \tag{20}$$

$$P_{SED} = P_{SCN} Y_{SED} ER \tag{21}$$

$$ER = m Y_{SED}^{y} T_f \tag{22}$$

Where

N_{SED}	nitrogen transported by sediment ($g\ s^{-1}$)
N_{SCN}	nitrogen content in soil (g per g soil). Similarly
P_{SED}	phosphorus transported by sediment ($g\ s^{-1}$)
P_{SCN}	phosphorus content in soil (g per g soil)
Y_{SED}	*s*ediment yield ($g\ s^{-1}$)
ER	nutrient enrichment function
m and y	are enrichment coefficients
T_f	correction factor for soil texture (e.g. 0.85 for sand, 1.0 silt, 1.15 for clay and 1.5 for peat).

3.3 River Nutrient Dynamics and Transport Model

The river nutrient module describes the in-stream nutrient dynamics and transport in a river network system using the dynamic equation of advection-dispersion with chemical reaction (Eq. 23) (Chapra 1997).

$$V\frac{\partial c}{\partial t} = \underbrace{\frac{\partial\left(A_c E \frac{\partial c}{\partial x}\right)}{\partial x}dx - \frac{\partial\left(A_c U c\right)}{\partial x}dx}_{Dispersion-Advection} + \underbrace{V(rc+p)}_{Reaction} + \underbrace{s}_{Sorce/Sink}$$

Where

V element volume
c nutrient concentration
A_c element cross-section area
E longitudinal dispersion coefficient
x along longitudinal space unit
t time
U average velocity
r reaction rate
p internal sources/sinks
s external or lateral sources/sinks.

The nutrient loads from each sub-catchment are used as input boundary conditions. The external input includes both inorganic and organic or soil bound nutrient from catchments.

3.3.1 Solution of Nutrient Transport Equation for River Network System

An explicit finite difference solution scheme was used to solve the mass balance Eq. (23) by discretizing the computational domain in space and time (Fig. 2) for calculation of nutrient concentration at each river grid. The explicit scheme is not as robust as an implicit scheme. However, the scheme is simple and easy to construct and computationally efficient. The results are affected by the scheme if the stability criteria are stratified. This was ensured in the model. The numerical form of the differential equation (Eq. 23) is shown in Eq. (24).

$$\frac{c_i^{n+1}-c_i^n}{\Delta t}=\frac{(A_cE)_{i,i+1}\left(c_{i+1}^n-c_i^n\right)}{V_i\Delta x}+\frac{(A_cE)_{i-1,i}\left(c_{i-1}^n-c_i^n\right)}{V_i\Delta x}+\frac{Q_{i-1}c_{i-1}^n-Q_ic_i^n}{V_i}+\left(r_ic_i^n+p_i\right)+\frac{s_i}{V_i} \quad (24)$$

By taking average of the cross-sectional area and dispersion coefficient E between interface grids *(i,i+ 1)* and *(i,i-1)* the Eq. (24) takes the form of Eq. (25), which achieves steady state condition in each time step to ensure model stability.

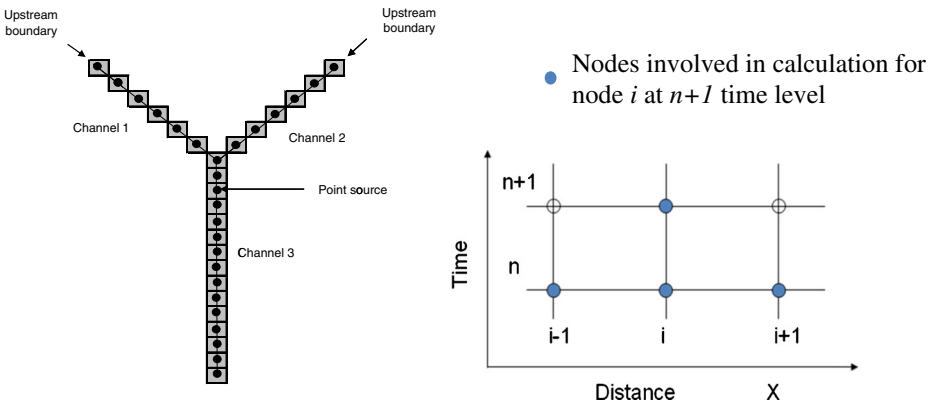

Fig. 2 Solution scheme for nutrient transport in branched network system

$$c_i^{n+1} = \frac{(A_c E)_{avg} c_{i+1}^n \Delta t}{V_i \Delta x} + c_i^n \left(1 - 2\frac{(A_c E)_{avg} \Delta t}{V_i \Delta x} - \frac{Q_i \Delta t}{V_i}\right) + c_{i-1}^n \left(\frac{(A_c E)_{avg} \Delta t}{V_i \Delta x} + \frac{Q_{i-1} \Delta t}{V_i}\right) - r_i c_i^n \Delta t + p_i \Delta t + \frac{s_i \Delta t}{V_i} \quad (25)$$

Where, negative sign denotes reaction component ($r_i c_i$) for decay.

The equation can be further re-arranged as:

$$c_i^{n+1} = c_{i+1}^n \lambda + c_i^n (1 - 2\lambda - \gamma) + c_{i-1}^n (\lambda + \gamma) - r_i c_i^n \Delta t + p_i \Delta t + \frac{s_i \Delta t}{V_i} \quad (26)$$

Where

λ Diffusion number = $\frac{(A_c E)_{avg} \Delta t}{V_i \Delta x}$

γ Advection number or Courant stability condition = $\frac{Q_i \Delta t}{V_i}$

In the model, longitudinal dispersion coefficient, E is calculated using the following equations developed by Fischer et al. (1979).

$$E = 0.011 \frac{U^2 W^2}{H U^*} \quad (27)$$

$$U^* = \sqrt{gHS_0} \quad (28)$$

Where

U Flow velocity m/s
W Channel width (m)
H Mean depth of water (m)
U^* Shear velocity (m s − 1)
g Acceleration due to gravity (m s − 2)
$S0$ Channel bed slope.

3.3.2 In-Stream Chemical Reactions

The term ($rc + p$) represents the reaction component in the mass balance Eq. (23), where rc is the total reactant, linearly dependant on the constituent's concentration and p represents the internal constituents - source and sink (Chapra 1997). Table 2 shows how these reaction terms (rc and p) have been represented for each constituent.

Figure 3 shows the chemical reaction process accounted in the model and the interaction between plant biomass (Algae) and sediment. The components of plant biomass and sediment interaction were not modelled due to non-availability of observed data in the selected study areas for model calibration and validation. Table 3 provides the list of state variables.

Table 2 Equations for in-stream reaction process (after Chapra 1997)

Constituent	Equations
Organic N (N_{ORG})	$\frac{dN_{ORG}}{dt} = \alpha_1\rho A - \beta_3 N_{ORG} - \sigma_4 N_{ORG}$ (27) The term $\alpha_1\rho A$ is accumulation due to algal respiration, where $\alpha_1\rho$ is accumulation rate of N_{ORG} due to algal respiration (day^{-1}) and A is mass of algae (mg l^{-1}), β_3 is decay coefficient of *ORG-N* and σ_4 is settling rate of N_{ORG}. The simulation of algal biomass can be carried out using following equation. $\frac{dA}{dt} = \mu A - \rho A - \frac{\sigma_1}{H}A$ (30) Where, μ is growth rate of algal biomass (day^{-1}), ρ is loss rate of algal biomass due to respiration, σ_1 settling rate of algae (m^{-1}) and H is water depth (m).
Ammonium N (N_{NH4})	$\frac{dN_{NH4}}{dt} = \beta_3 N_{ORG} - \beta_1 N_{NH4} + \frac{\sigma_3}{H} N_{NH4} - F\alpha_1\mu N_{NH4}$ (31) Where, β_3 is decay rate of *ORG-N*, β_1 is rate of nitrification of N_{NH4}, σ3 is accumulation rate of N_{NH4} due to resuspension of sediment, $F\alpha_1\mu N_{NH4}$ is total loss of N_{NH4} for algal growth, $\alpha_1\mu$ is loss rate of N_{NH4} for algal growth and F is fraction.
Nitrite N (N_{NO2})	$\frac{dN_{NO2}}{dt} = \beta_1 N_{NH4} - \beta_2 N_{NO2}$ (32) where, β_2 is rate of nitrification of N_{NO2}
Nitrate N (N_{NO3})	$\frac{dN_{NO3}}{dt} = \beta_2 N_{NO2} - (1-F)\alpha_1\mu N_{NO3}$ (33)
Organic P (P_{ORG})	$\frac{dP_{ORG}}{dt} = \alpha_2\rho A - \beta_4 P_{ORG} - \sigma_5 P_{ORG}$ (34) where, $\alpha_2\rho$ is rate of accumulation of P_{ORG} due to algal respiration, β_4 is a decay rate of P_{ORG}, σ_5 is settling rate of P_{ORG}
Dissolved P (P_{DISS})	$\frac{dP_{DISS}}{dt} = \beta_4 P_{ORG} + \frac{\sigma_2}{H} P_{DISS} - {}^{DISS}\alpha_2\mu P_{DISS}$ (35) where, β_4 decay rate of P_{ORG}, σ_2 is accumulation rate of P_{DISS} due to re-suspension of sediment, $\alpha_2\mu$ loss rate of P_{DISS} for algal growth.

4 Study Areas

4.1 The Saru River Basin

The Saru River is situated in Hokkaido, which is in the northernmost area of Japan (Fig. 4a). It originates at Mount Memuro (Nakamura and Kikuchi 1996) and passes through an alluvium plain in the downstream region, and has a catchment area of 1,350 km^2. With a trunk river channel length of 104 km and a bed slope ranging from 1/500 to 1/800, it is one of the steepest river systems in this region of Japan (Yoshikawa et al. 2006). The basin is known as rocky, with a thin top soil layer (about 1 m) (Yoshikawa et al. 2006). The land use is predominantly forest (92 %). Other land use types are agriculture including rice, fruits and vegetable growing fields, and some urban features.

Flooding is a recurring phenomenon in the Saru River. Huge amounts of sediment and nutrients were carried out by the river during heavy floods in 2001. Water quality measurements of these two flood events in the basin were used for the model calibration and validation.

4.2 The Latrobe River Basin

In contrast, the Latrobe River is situated in a very dry temperate region of the Victorian State in Australia. It drains a catchment area of 4,500 km^2 (Fig. 4b). The river has significant socio-economic and environmental values for the region, which is used for supplying water to some major thermal electric power generation plants and other

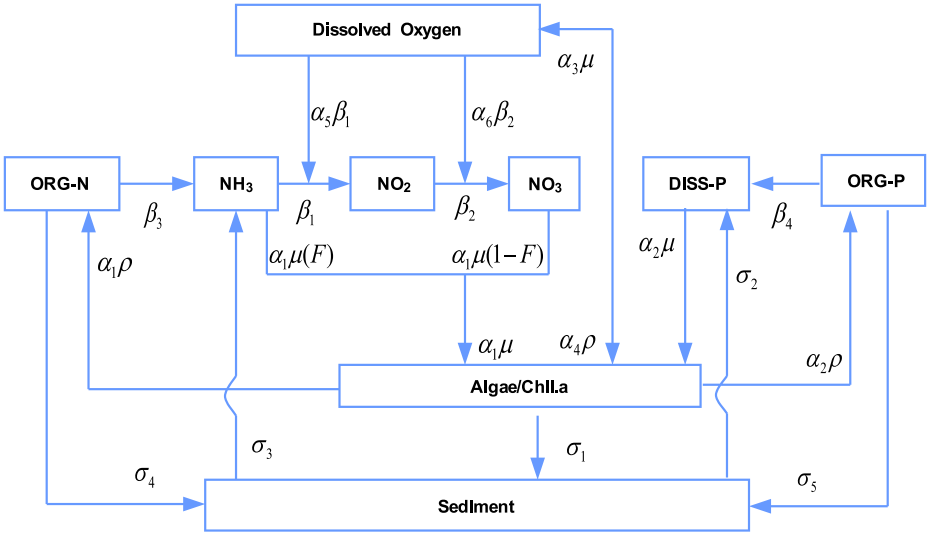

Fig. 3 In-stream chemical reaction with plant-sediment-nutrient interaction (modified from Chapra 1997)

regional industries (LVWSB 1986). The land use types are mainly forest (41 %), dairy farm (44 %), natural grazing pasture, mining and cropping land. Built up areas are relatively small.

The upper and relatively hilly catchment is selected for modelling. The river originates on a hilltop and incises through the undulating landscape before steps down to relatively flat area from topographic elevation 274 to 59 m. The land use types are mainly production forest and grazing pasture in this upper catchment.

5 Modelling in the Saru River Basin

5.1 Model Setup

The original 250-m grid of Digital Elevation Model (DEM) for the study area was hydrologically corrected using the hydrological assessment tool within ARCGIS. The river network was derived from the corrected DEM using GIS to form the river model. Each branch of the river network was indexed and every node was defined with cross-section geometry. The catchment was divided into 17 sub-catchments coinciding the inflow nodes from 17 branches to main trunk of the river network.

Table 3 Model state variables

1) Plant uptake of nitrogen	8) Plant uptake of *P*
2) Organic *N* (N_{ORG})	9) Organic *P* (P_{ORG})
3) Net mineralization of *P*	10) Net mineralization of *P*
4) Net nitrification of *N*	11) Phosphate *P* (PO_4-*P* or P_{DISS})
5) Net denitrification of *N*	12) Suspended sediment
6) Ammonium *N* (N_{NH4})	
7) Nitrite + Nitrate *N*	

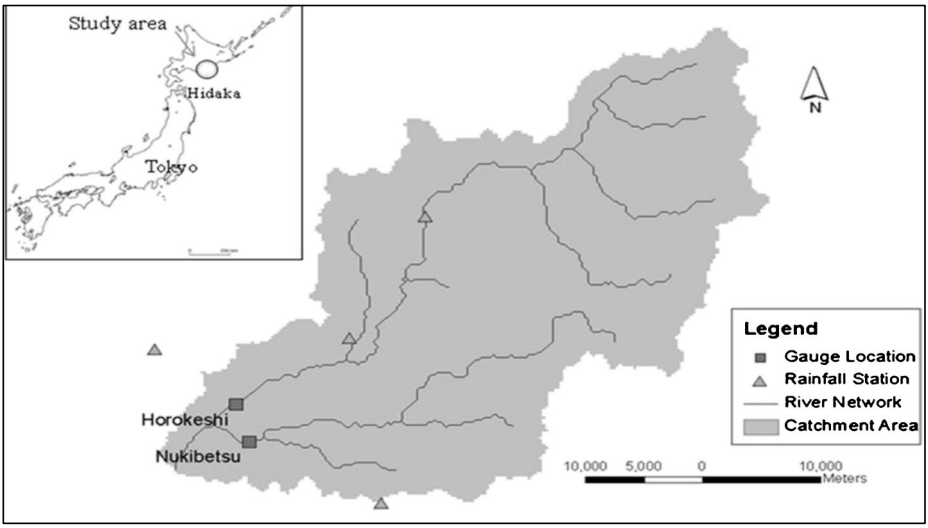

(a) Saru River Basin

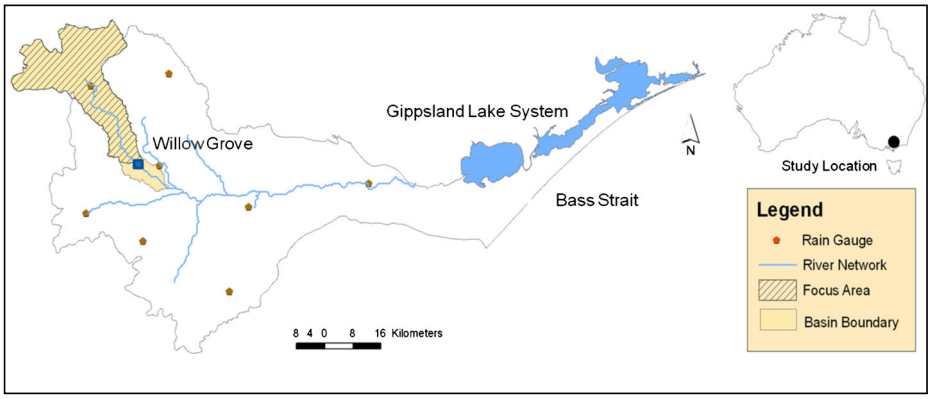

(b) Latrobe River basin

Fig. 4 Study areas in the **a** the Saru River basin and **b** Latrobe River Basin

The time series inputs were hourly rainfall and daily evaporation data for hydrological simulation. The RUSLE method was used to estimate soil erosion. Based on the sediment delivery ratio the sediment yield was predicted. The K factor was assumed for sandy layer of the top soil of the catchment. LS parameter depends on the slope length and steepness of the sub-catchments. C_m and P_s factors are the average value for the different land use types. The suspended sediment measured at Horokeshi station for three consecutive days during the flood event was used for comparison with the model results.

The calculation of nutrient release from sub-catchments involves estimation of organic and inorganic nutrients. The soil bound organic nutrient was estimated as sediment yield multiplied with nutrient concentration in eroded soil. The inorganic nutrient release was estimated based on different input rates of nutrient generation and transformation. The input rate of N and P mineralization from different land uses and their corresponding

transformation rates were obtained from literature such as Whitehead et al. (1998b). However, the information is very scarce for the *P* process. The observed *P* uptake rate for different crops and grassland for the catchments of UK and USA as reported in Wade et al. (2007) has been used as a guide for determining *P* uptake rate. The details of the input parameters are also provided in Table 4.

The *SMI* was assumed to be at constant level 1, considering the wet/saturated condition of the catchment during the flood events. The effect of *SMI* over short period would not change. The reaction coefficients in the river module were judged based on available information in the text book of Chapra (1997).

5.2 Model Accuracy and Sensitivity Analysis

An assessment of numerical accuracy and sensitivity analysis of model parameters were undertaken prior to the model calibration and validation. A parameter perturbation method was used for the sensitivity analysis. The numerical accuracy was assessed by analyzing mass balance and verifying the stability criteria. The numerical stability criteria of the Courant condition and the Diffusion number were estimated during simulation, which should be less than 1 and 0.5, respectively at each time step. For mass balance, a test simulation was carried out using synthetic time series boundary conditions applied at each upstream point of the Saru River network. The constituent model was run without chemical reaction. The simulated results had 8 % and 6 % numerical errors for *N* and *P,* respectively, and less than 4 % for discharge. These errors margins of less than 10 % are considered to be acceptable. The difference in error for *N* and *P* was mainly due to the difference in magnitude for input loadings.

The sensitivity tests suggest that the chemical reaction coefficients have a significant impact on the nutrient level at river network system and these are to be judged during calibration process. The export coefficients of surface model have high impacts on nutrient loading, which are also to be judged during calibration. It is noteworthy to mention that the adequacy of organic nutrient loading calculation depends on the calibration of the sediment modelling and assumption of nutrient content in eroded soil.

Table 4 Input for catchment nutrient process modelling

Input	Latrobe River		Saru River		
	Grazing pasture	Production Forest	Paddy Field	Grassland	Forest
N Fertilizer (kg ha^{-1} year^{-1})	60	–	150	–	–
N Uptake (kg ha^{-1} year^{-1})	35	5	95	35	40
N Mineralization (kg ha^{-1} year^{-1})	60	40	50	40	40
Nitrification (kg ha^{-1} year^{-1})	20	10	30	15	15
Denitrification (kg ha^{-1} year^{-1})	1	1	19	1	1–4
P Uptake (kg ha^{-1} year^{-1})	12	–	25	12	–
P Mineralization (kg ha^{-1} year^{-1})	12	10	0	0	0
P Fertilizer (kg ha^{-1} year^{-1})	44	0	70	23	0

5.3 Model Calibration and Validation

The model was calibrated against observed streamflow and sediment and nutrient fluxes. The calibration was first undertaken against streamflow using Manning's roughness coefficient for both overland and river flow. An extreme flood event in September 2001 was used for the calibration. A relatively lower magnitude flood event occurred during August 2001 was selected for model validation. These two flood events were selected due to the availability of high quality observed data of suspended sediment and nutrient fluxes, collected by intensive field sampling during the flood events. The calibrated parameters were used in the validation without any further adjustment. The model results were compared against the observed records for evaluating performance using a number of statistical evaluation criteria (Van Liew et al. 2005 and Stehr et al. 2008) (Table 5).

5.4 Results

(a) Hydrological simulation results

The hydrological simulation was carried out for generating catchment runoff and river discharges. The comparisons of the observed and simulated discharges at Horokeshi station during the calibration and validation are shown in Fig. 5a and b, respectively. The peak flow and the overall shape of the hydrographs match very well with the observed data during the period of calibration. The model performance was similar in the validation period as well. The *NSE* values were 0.87 and 0.94 for the calibration and validation periods, respectively (Table 6).

(b) The soil erosion and sediment yield

The samples of suspended sediments during the field measure were taken in varied intervals ranging from 15 min to a few hours. The data was averaged to daily interval and compared with the RUSLE model output as shown in Fig. 5c and d. The simulated time series of suspended sediments show close agreement with the observed data for both calibration and validation periods. Although number of observed data were limited, the agreement between the observed data and simulated results was highly satisfactory.

(c) Nutrient simulation results

The observed data were available in the form of total nitrogen (*TN*), NH_4 and NO_3 and total phosphorus (*TP*), PO_4 and dissolved phosphate (DPO_4). From these datasets, organic *N* and *P* were derived as a difference between total and inorganic *N* and *P*, respectively. The interval of data varied from 15 min to few hours for consecutive 3 days during each of the two flood events in August and September 2001. The 15-min interval data was averaged to hourly interval and compared with the model results.

The model computes nutrient concentration at each node of the river network system. The results were compared with the observed nutrient records at Horokeshi gauge and

Table 5 Evaluating criteria for model results against statistical indices

	Good	Satisfactory	Not satisfactory
NSE	>0.75	0.75–0.36	<0.36
Correlation coefficient (R^2)	>0.75	0.75–0.36	<0.36
PBIAS (percentage of biasness)	<±20 %	±20–±40	<±40

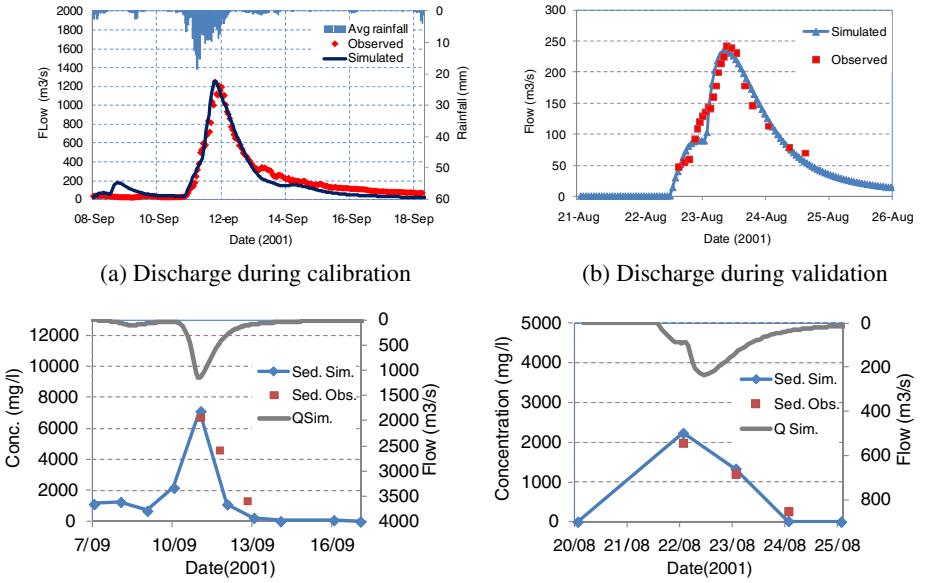

(a) Discharge during calibration

(b) Discharge during validation

(c) Suspended sediment during calibration

(d) Suspended sediment during validation

Fig. 5 Comparison of simulated and observed discharge and suspended sediments during calibration and validation at Horokeshi, the Saru River

presented with stream flow in the same plot for showing the relationship between the streamflow flow and nutrient fluxes.

Figure 6a–d compares the simulated and observed nutrient levels in the Saru River during calibration. The simulated results agreed well with the observed data. The profiles of *ORG-N* and *ORG-P* show the rise and fall varying with the stream flow indicating strong co-relation between river flow and nutrient loads. The initial condition was set to zero level from where the concentration was rising with the increase of nutrient loading from the sub-catchments and started decreasing with the

Table 6 Statistical indices evaluating model performance for the Saru River

Simulation Period	Parameter	*RRMSE*	*MAE*	*PBIAS*	*NSE*	R^2
Sep 2001	*Flow*	0.31	55.97	7.47	0.94	0.95
	Sus.sed (SS)	0.50	1668.13	33.00	0.80	0.80
	ORG-N	0.24	2.04	−18.07	0.70	0.73
	NO_3-*N*	0.05	0.02	1.00	0.67	0.60
	ORG-P	0.23	0.34	−17.98	0.72	0.79
	$P0_4$-*P*	0.17	0.23	−6.96	0.78	0.66
Aug 2001	*Flow*	0.15	17.74	1.34	0.87	0.90
	Sus.sed	0.19	205.99	−3.51	0.98	0.99
	ORG-N	0.12	0.08	0.51	0.42	0.87
	NO_3-*N*	0.03	0.01	1.81	0.47	0.60
	ORG-P	0.19	0.04	6.99	0.52	0.57
	PO_4-*P*	0.17	0.03	−12.52	0.69	0.82

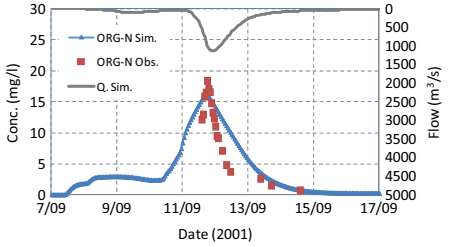

(a) ORG-N during calibration

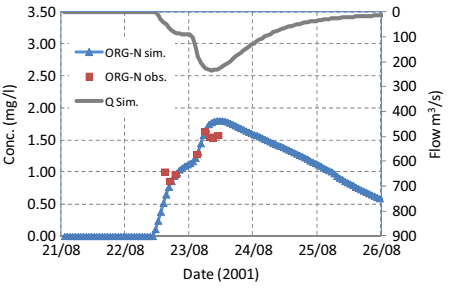

(b) ORG-N during validation

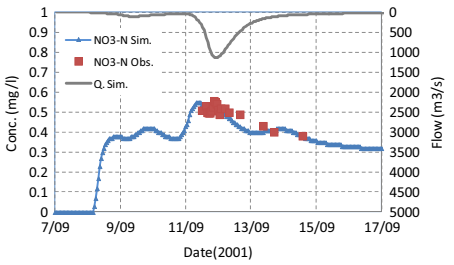

(c) NO_3-N during calibration

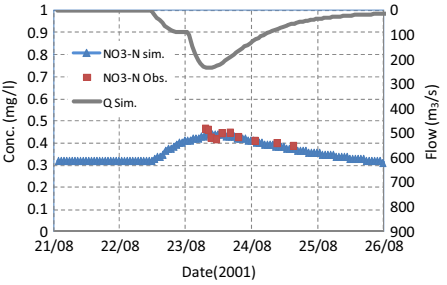

(d) NO_3-N during validation

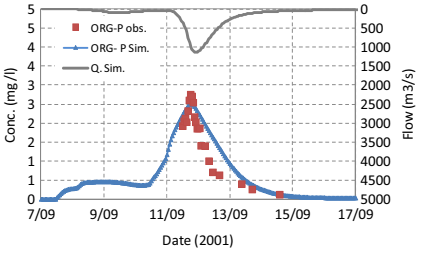

(e) ORG-P during calibration

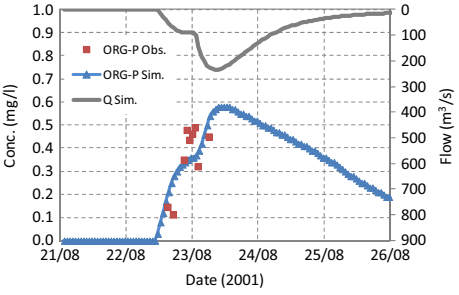

(f) ORG-P during validation

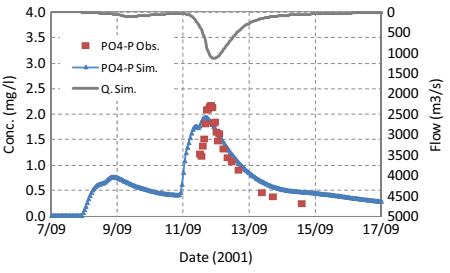

(g) PO_4-P during calibration

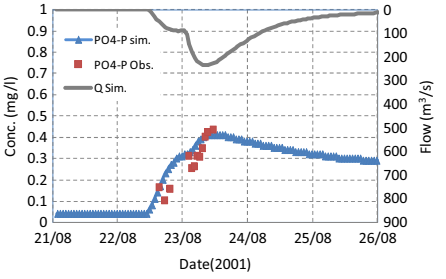

(h) PO_4-P during validation

Fig. 6 Comparison of simulated and observed nutrients at Horokeshi during the periods of model calibration and validation

decrease of flow. The high intensity flood carried out huge wash off pollutant as reflected in the figure. Due to decay of NO_3-N the profile was flattened, which agreed well with the observed pattern. The model performance level was in the range from the "satisfactory" to the "good" level as presented in Table 6. The *NSE* and R^2 values are above 0.69 and 0.60 with the maximum values 0.77 and 0.79, respectively during calibration.

The model set up for the validation was same as the calibration except the period of simulation. The initial conditions for nutrient concentration at each river grids were set to zero for most of the pollutants. The simulated nutrient fluxes are presented in Fig. 6e–h along with the observed data. The results show the rising limbs match well with the observed data for *ORG-N* and *ORG-P* and PO_4-P. The response of chemical reaction is seen on the concentration level of NO_3-N and PO_4-P, which shows the gradual decrease of NO_3-N and PO_4-P levels at recession limbs. The model performance is within the range of satisfactory and good levels (Table 6). The concentration level of NO_3-N matched well with the observed data in the recession limb of the hydrograph with *NSE* and R^2 values of 0.47 and 0.6, which are satisfactory. The *PBIAS* value is within the good range for all nutrient constituents in the calibration and validation.

6 Modelling in the Latrobe River

6.1 Model Set Up

A 1-km DEM was used to set up the hydrological model for the Latrobe River. The model also consists of the land use and soil maps. The model was calibrated against Manning's roughness parameter. A runoff coefficient was used in determining surface runoff and a constant base flow was assumed to match the low flow, which is 1.9 m^3s^{-1}. For the Latrobe River basin, the simulation was carried out for a longer period. The data preparation for this application was similar to the Saru River application. The MUSLE was used for continuous simulation of sediment yield. Average K value was assumed for soil types of the catchment. C_m and P_s factors were assumed for the different land use types mainly forests and pasture. The input parameters for nutrient flux simulation are tabulated in Table 4 above. For pasture based grazing system the P application rate is 44 kg ha^{-1} $year^{-1}$ in the Latrobe river region (Drysdale 1998; Nash and Halliwell 1999). The N application rate is from previous reference. The yearly input rate of fertilizer was uniformly distributed over the simulation period. A further analysis

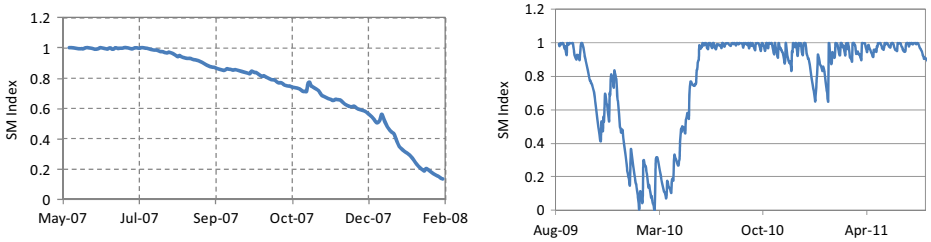

Fig. 7 Soil moisture index for the Latrobe River

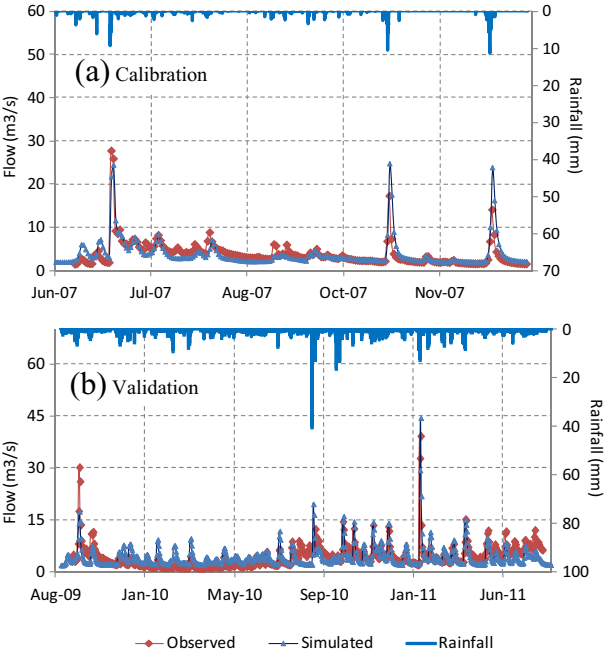

Fig. 8 Comparison of discharge at Willow Grove, the Latrobe River

on actual timing of fertilizer application is needed. The soil moisture index (SMI) was calculated based on rainfall, runoff and antecedent soil moisture condition. Figure 7 shows the seasonal variation of *SMI* index for the Latrobe River.

6.2 Model Calibration and Validation

The hydrological model was first calibrated using Manning's roughness parameter and then, the sediment and nutrient modules were calibrated. A runoff coefficient was used in determining surface runoff and a constant base flow was assumed to match the low flow, which is 1.9 m^3s^{-1}. The validation period was from September 2009 to end of July 2011.

Table 7 Statistical indices for hydrological, sediment and nutrient model results at Willow Grove, the Latrobe River

Parameters	Period	*RRMSE*	*MAE*	*PBIAS*	*NSE*	R^2
Discharge	Calibration	0.48	1.05	−3.00	0.66	0.74
	Validation	0.55	1.79	−2.40	0.51	0.55
Sus.Sed	Calibration	0.25	1.94	8.77	−0.10	0.04
	Validation	0.57	4.26	30.61	−0.23	0.53
ORG-N	Calibration	0.30	0.07	19.84	−0.73	0.01
	Validation	0.59	0.15	36.95	−0.39	0.29
TP	Calibration	0.38	0.01	20.41	−0.29	0.45
	Validation	0.49	0.01	30.38	−0.22	0.52
NO_3-*N*	Calibration	0.18	0.05	−1.88	0.76	0.77
	Validation	0.33	0.00	9.09	0.43	0.60

6.3 Results

(a) Hydrological model results

Figure 8 shows a comparison of the simulated and observed discharge at Willow Grove. By statistical measures the model shows satisfactory performance (Table 7). The *NSE* values are 0.66 and 0.51 and R^2 values 0.74 and 0.55 for the calibration and validation periods, respectively.

(b) Sediment modelling results

Figure 9a–b shows the comparison of the observed sediment and MUSLE model

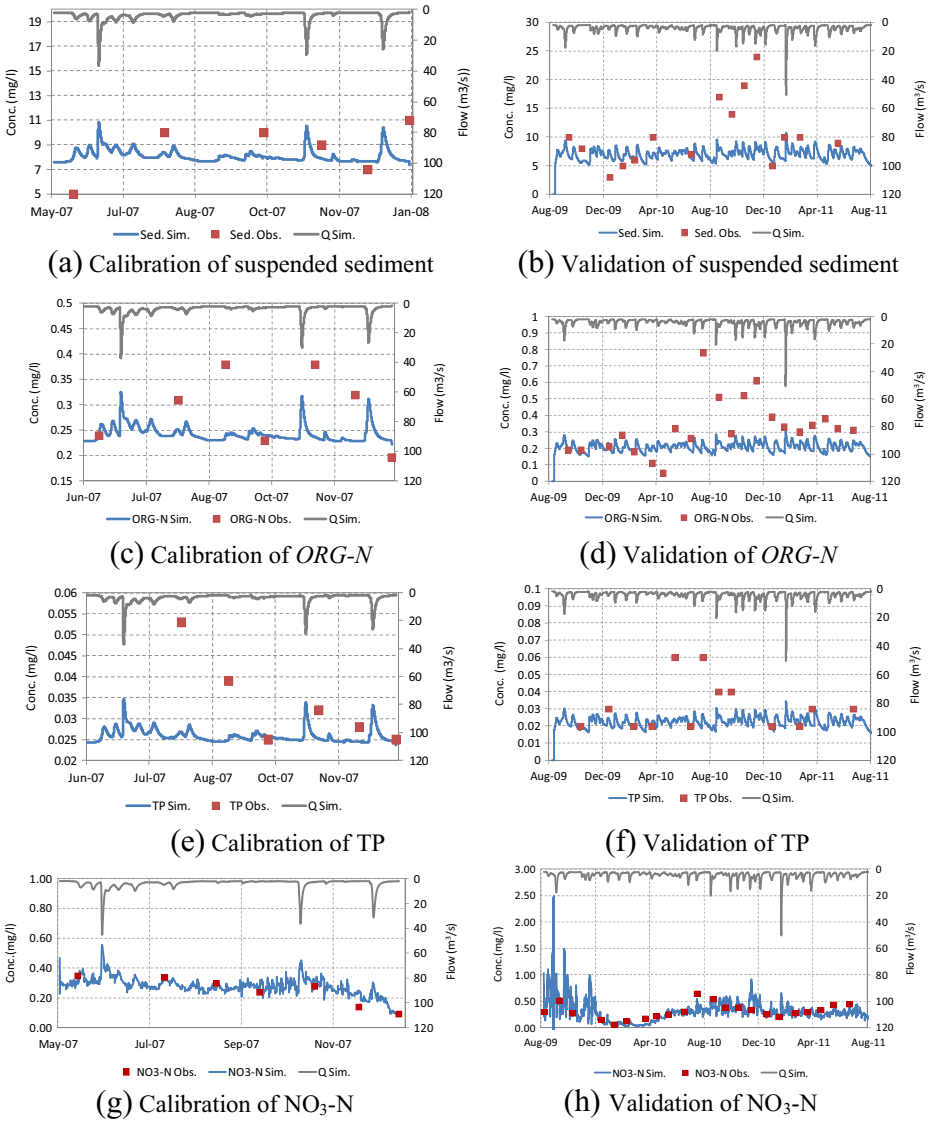

(a) Calibration of suspended sediment

(b) Validation of suspended sediment

(c) Calibration of *ORG-N*

(d) Validation of *ORG-N*

(e) Calibration of TP

(f) Validation of TP

(g) Calibration of NO_3-N

(h) Validation of NO_3-N

Fig. 9 Comparison of observed and simulated suspended sediment, ORG-N, TP and NO_3-N at Willow Grove, the Latrobe River during the model calibration and validation

results at Willow Grove with the statistics presented in Table 7. The sediment concentration is highly correlated to the discharge. However, there was not enough dataset to compare the model results particularly for the period of calibration. The results in the validation period are within the upper and lower range of the observed data with few observed data points outside of the range.

(c) Nutrient modelling results

Figures 9c–f show the comparison of model results for *ORG-N* and *TP*. The model results could only follow the overall trend in observed *ORG-N* and *TP* level. The observed data is scattered, hence, a good performance could not be achieved by statistical measures (Table 7). The levels of *ORG-N* and *TP* are dependent on the level of sediment yield, both cases represent similar trend (Fig. 9).

The seasonal pattern of NO_3-*N* level was predicted reasonably accurately by the model (Fig. 9g–h)). The *NSE* and R^2 values during the calibration period are 0.76 and 0.77, respectively and those were 0.4 and 0.6, respectively for the validation.

7 Discussion

The model performed reasonably well in two different catchments demonstrating its ability to predict the nutrient levels under different hydro-climatic conditions. With the adequate mathematical representations of soil erosion and transport, and nutrient generation and transport along the hydrological flow paths within a process-based hydrological modelling framework, the model was able to simulate the sediment and nutrient fluxes reasonably well in high flow events. The high intensity measurements in the Saru River were useful to evaluate the adequacy of sediment and nutrient modelling in high intensity storm events. The model was also able to simulate long term seasonal pattern of sediment and nutrient levels in the Latrobe River.

The separation of nutrient generation process and transport in the modelling process has been effective in determining the different forms of nutrients loads including the sediment bound nutrients. Table 8 shows the contribution of nutrient from different components. From this table, it is seen that the organic loads are usually higher than inorganic loads in the Saru River but in the upper catchment of the Latrobe river the inorganic *N* load is higher than soil bound organic *N*, which is due to the fact that huge amount of sediment and nutrient loads were washed off during the high intensity storm events in the Saru River, whereas in Latrobe River the wash-off loads were relatively low.

Process-based nutrient models are generally complex relying on a large number of datasets. However, we could gather reasonably high intensity field measured data particularly for the Saru River to validate the model in predicting nutrient release in

Table 8 Total nutrient loads from different components

	Period	Organic N Load	Inorganic N load (kg)	Organic P Load	Inorganic P load (kg)
Saru River	Calibration	1466430	65697	229379	190813
	Validation	39819	11144	12742	9828
Upper Latrobe	Calibration	18725	23527	1997	–
	Validation	35572	92986	3794	–

higher resolution. With the improvements in monitoring techniques, sampling methods and analysis techniques in the recent years, the quality and resolution of data required for such modelling are becoming available.

The study suggests that the soil erosion models can be further improved. Using soil delivery ratio is a relatively simple way to predict sediment dynamics. The ratio is a function of length, slope and a constant, which is a conceptual approach in deriving yield without accounting actual catchment process. The RUSLE method was replaced by MUSLE for the Latrobe River to take into account of overland flow effects on soil erosion and provide continuous output of sediment yield. The MUSLE is found to be more effective than RUSLE. However, this could be improved further if the hill slope soil erosion is coupled with sediment transport modelling. There is a scope to improve this component of the model in the future research.

8 Conclusion

We have presented the development and applications of a sub-catchment based nutrient model. The model accounts the processes of internal chemical reaction with soil-moisture and climate condition in estimating nutrient generation and release from different land uses. A function based approach was introduced to estimate dissolved nutrient release with runoff. Widely used empirical methods for soil erosion and sediment yield was used to estimate soil bound nutrient. The performance of the model in calibration and validation was quite acceptable for the two case studies. The model was able to predict the nutrient fluxes association with two short term record breaking flood events in the Saru River and the long term nutrient level in the Latrobe River. The model could provide output at an hourly interval, which was validated against observed data, showing realistic details of the nutrient dynamics. The statistical indices show satisfactory and good level performance for the Saru River. In spite of limited data, the model could reproduce the seasonal trend of nutrient level for the Latrobe River reasonably well. However, due to poor performance of sediment model, the actual profile of soil bond *TP* and *ORG-N* could not be predicted well for the Latrobe River. There is a scope to improve the model by replacing the empirical approach with process oriented sediment modelling approach.

The study has shown that the nutrient model is suitable for predicting actual nutrient pollution in rivers. By simulating organic and inorganic nutrients separately the actual river water quality status could be known effectively. The application of the model can be extended to incorporate other pollutants such as bacteria.

Acknowledgements Authors greatly acknowledge the Civil Engineering Research Institute of Hokkaido and Kitami Institute of Technology, Japan and Victorian Water Resources Database for data and several internal and external reviewers for their contribution to improve the manuscript.

Compliance with Ethical Standards

Funding The study was undertaken as part of a PhD research project at Monash University, Australia and partially funded by the Asia Pacific Network for Global Change Research.

Conflict of Interest The authors declare that they have no conflict of interest.

References

Abbott MB, Bathurst JC, Cunge JA, O'Connell PE, Rasmussen J (1986) An introduction to the European hydrological system - systeme hydrologique Europeen, 'SHE', 2: structure of a physically-based, distributed modelling system. J Hydrol 86:61–77

Abrahamsen P, Hansen S (2000) Daisy: an open soil-crop-atmosphere system model. Environ Model Softw 15:313–330

Alam MJ, Dutta D (2013) Predicting climate change impact on nutrient pollution in waterways: a case study in the upper catchment of the Latrobe River, Australia. Ecohydrology 6(1):73–82

Arnold JG, Srinivasan R, Muttiah RS, Williams JR (1998) Large area hydrologic modeling and assessment: part I. Model development. J Am Water Resour Assoc 34(1):73–89

Asokan S, Dutta D (2008) Analysis of water resources in the Mahanadi River Basin, India under projected climate conditions. Hydrol Process 22:3589–3603

Bhattarai R, Dutta D (2007) Estimation of soil erosion and sediment yield using GIS at catchment scale. Water Resources Management Journal 21:1635–1647

Bhattarai R, Dutta D (2008) A comparative analysis of sediment yield simulation by empirical and process-oriented models in Thailand. Hydrol Sci J 53(6):1253–1269

Chapra SC (1997) Surface-water quality modelling. WCB McGraw Hill, USA

Chau KW, Wu CL (2010) A hybrid model coupled with singular spectrum analysis for daily rainfall prediction. J Hydroinf 12(4):458–473

Chen XY, Chau KW, Wang WC (2015) A novel hybrid neural network based on continuity equation and fuzzy pattern-recognition for downstream daily river discharge forecasting. J Hydroinf 17(5):733–744

Chow VT, Maidment DR, Mays LW (1988) Applied hydrology, McGrawhill, USA

Cook FJ, Jordan PW, Waters DK, Rahman JM (2009) WaterCAST – Whole of catchment hydrology model an overview. MODSIM Congress, Cairns

Croke J (2002) Managing phosphorus in catchment, River Landscapes, Fact Sheet 11, Land & Water, Australia

Croke J, Young B (2001) River contaminants: what are river contaminants and how can we effectively manage them for riverine and ecosystem protection? "RipRap", River and Riparian Lands Management Newsletter, Land & Water Australia, Canberra, 20:1–6

DHI (2002) MIKE11: A modelling system for rivers and channels, Reference manual, DHI Water & Environment, Hørsholm, Denmark

Dise N (2004) An introduction to INCA: integrating nitrogen in catchment. Hydrol Earth Syst Sci 8(4):597–600

Drysdale G (1998) Dairy farm performance analysis 1996–97. Annual Report, DNRE, Melbourne

Dutta D, Nakayama K (2009) Effects of spatial grid resolution on river flow and surface inundation simulation by physically based distributed modelling approach. Hydrol Process 23:534–545

Dutta D, Das Gupta A, Ramnarong V (1998) Design and optimisation of a groundwater monitoring system. Ground Water Monit Remediat 18(1):139–147

Dutta D, Herath S, Musiake K (2000) Flood inundation simulation in a river basin using a physically based distributed hydrologic model. Hydrol Process 14:497–519

Dutta D, Herath S, Musiake K (2006) An application of a flood risk analysis system for impact analysis of a flood control plan in a river basin. Hydrol Process 20(6):1365–1384

Finkele K, Mills GA, Beard G, Jones DA (2006) National gridded drought factors and comparison of two soil moisture deficit formulations used in prediction of forest fire danger index in Australia. Aust Meteorol Mag 55:183–197

Fischer HB, List EJ, Koh RCY, Imberger J, Brooks NH (1979) Mixing in inland and coastal water. Academic, New York

Guse B, Pfannerstill M, Fohrer N (2015) Dynamic modelling of land use change impacts on nitrate loads in rivers. Environ Process 2(4):575–592

Hansen S, Jensen HE, Nielson NE, Svendson H (1990) DAISY. A soil plant system model. Danish simulation model for transformation and transport of energy and matter in the soil plant atmosphere system. NPO-Research Report A 10, Copenhagen

Jha R, Herath S, Musiake K (2000) River network solution for a distributed hydrological model and applications. Hydrol Process 14:575–592

Jones CA, Dyke PT, Williams JR, Kiniry JR, Benson VW, Griggs RH (1991) EPIC: an operational model for the evaluation of agricultural sustainability. Agric Syst 37:341–350

Kabir MA, Dutta D, Hironaka S (2011) Process-based distributed modelling approach for analysis of sediment dynamics in a River Basin. J Hydrol Earth Syst Sci 15(4):1307–1321

Kouwen N (1999) WATFLOOD/SPL8 Flood Forecasting System. Documentation and User Manual. Civil Engineering, University of Waterloo, Waterloo, Canada

Leon LF, Soulis ED, Kouwen N, Farquhar GJ (2001) Nonpoint source pollution: a distributed water quality modelling approach. Water Res 35(4):997–1007

Lunn RJ, Adams R, Mackay R, Dunn SM (1996) Development and application of a nitrogen modelling system for large catchments. J Hydrol 174:285–304

LVWSB (1986) The Latrobe River Basin, Water Resources and Aquatic Environment, a review, The Latrobe Valley Water and Sewerage Board, Australia

Nakamura F, Kikuchi S (1996) Some methodological development in the analysis of sediment transport process using age distribution of floodplain deposits. Geomorphology 16:139–145

Nash DM, Halliwell DJ (1999) Fertilisers and phosphorus loss from productive grazing systems. Aust J Soil Res 37:403–429

Panagopoulos Y, Makropoulos C, Mimikou M (2011) Diffuse surface water pollution: driving factors for different Geoclimatic regions. Water Resour Manag 25:3635–3660

Perraud JM, Seaton SP, Rahman JM, Davis GP, Argent RM, Podger GM (2005) The architecture of the E2 catchment modelling framework, MODSIM2005, 690–696

Radwan M, Willems P, El-Sadek A, Berlamont J (2003) Modelling of dissolved oxygen and biochemical oxygen demand in river water using a detailed and a simplified model. River Basin Manag 1(2):97–103

Refsgaard JC, Thorsen M, Jensen JB, Kleeschulte S, Hansen S (1999) Large scale modelling of groundwater contamination from nitrate leaching. J Hydrol 211:117–140

Renard KG, Foster GR, Weesies GA, Porter JP (1991) RUSLE, revised universal soil loss equation. J Soil Water Conserv 46(1):30–33

Renard KG, Foster GR, Weesies GA, McCool DK, Yoder DC (1996) Predicting soil erosion by water: a guide to conservation planning with the Revised Universal Soil Loss Equation, US Department of Agriculture, Agricultural handbook, 703

Saeidifarzad B, Nourani V, Aalami MT, Chau KW (2015) Multi-site calibration of linear reservoir based geomorphologic rainfall-runoff models. Water 6:2690–2716, 2014

Stehr A, Debels P, Romero F, Alcayaga H (2008) Hydrological modelling with SWAT under conditions of limited data availability: evaluation of results from a Chilean case study. Hydrol Sci J 53(3):588–601

Taormina R, Chau KW (2015) Neural Network River forecasting with multi-objective fully informed particle swarm optimization. J Hydroinf 17(1):99–113

Tzoraki OA, Dörflinger G, Kathijotes N, Kontou A (2014) Nutrient-based ecological consider-ation of a temporary river catchment affected by a reservoir operation to facilitate efficient management. Water Sci Technol 69(4):847–854

Van Liew MW, Arnold JG, Bosch DD (2005) Problems and potential of auto calibrating a hydrologic model. Trans ASAE 48(3):1025–1040

Venohr M, Hirt U et al (2011) Modelling of nutrient emissions in river systems - MONERIS - methods and background. Int Rev Hydrobiol 96(5):435–483

Wade AJ, Whitehead PG, Butterfield D (2002) The integrated catchments model of phosphorus dynamics (INCA-P), a new approach for multiple source assessment in heterogeneous river systems: model structure and equations. Hydrol Earth Syst Sci 6(3):583–606

Wade AJ, Butterfield D, Griffiths T, Whitehead PG (2007) Eutrophication control in river systems: an application of INCA-P to the River Lugg. Hydrol Earth Syst Sci 11(1):584–600

Wagenschein D, Rode M (2008) Modelling the impact of river morphology on nitrogen retention. Ecol Model 211:224–232

Wang H, Wu Z, Hu C (2015a) A comprehensive study of the effect of input data on hydrology and non-point source pollution modelling. Water Resour Manag 29(5):1505–1521

Wang WC, Chau KW, Xu DM (2015b) Improving forecasting accuracy of annual runoff time series using ARIMA based on EEMD decomposition. Water Resour Manag 29(8):2655–2675

Weischmer WH, Smith DD (1978) Predicting rainfall erosion losses - a guide to conservation planning, USDA. Agricultural Handbook, p 282

Whitehead PG, Wilson EJ, Butterfield D (1998) A semi-distributed integrated nitrogen model for multiple source assessment in catchment, Part I. model structure and process equations. The Science of the Total Environment. 210/211:547–558

Whitehead PG, Wilson EJ, Butterfield D, Seed K (1998) A semi-distributed integrated flow and nitrogen model for multiple source assessment in catchments (INCA): Part II- application to large river basins in South Wales and Eastern England. The Science of the Total Environment, 210/211:559–83

Williams JR (1975) Sediment-yield prediction with universal equation using runoff energy factor. present and prospective technology for predicting sediment yields and sources, ARS-S-40. USDA. Agric Res Serv 244–252

Williams JR, Berndt HD (1977) Sediment yield prediction based on watershed hydrology. Trans Am Soc Agric Eng 20:1100–1104

Wu G, Xu Z (2011) Prediction of algal blooming using EFDC model: case study in the daoxiang Lake. Ecol Model 222:1245–1252

Wu CL, Chau KW, Li YS (2009) Methods to improve neural network performance in daily flows prediction. J Hydrol 372(1–4):80–93

Yoshikawa Y, Yasuda H, Watanabe Y, Nakayama K, Dutta D (2006) Sediment transport during flood and application of distributed hydrological model. APHWR conference. (ST1-01-A06-119-), 1–8